Loughborough University

This item was submitted to Loughborough's Research Repository by the author.
Items in Figshare are protected by copyright, with all rights reserved, unless otherwise indicated.

A European proficiency test on thin-film tandem photovoltaic devices

PLEASE CITE THE PUBLISHED VERSION

https://doi.org/10.1002/pip.3322

PUBLISHER

John Wiley & Sons Ltd

VERSION

VoR (Version of Record)

PUBLISHER STATEMENT

This is an Open Access Article. It is published by Wiley under the Creative Commons Attribution 4.0 International Licence (CC BY 4.0). Full details of this licence are available at: https://creativecommons.org/licenses/by/4.0/

LICENCE

CC BY 4.0

REPOSITORY RECORD

Salis, Elena, Andreas Gerber, Jens Wenzel Andreasen, Suren A. Gevorgyan, Tom Betts, Blagovest Mihaylov, Ralph Gottschalg, et al.. 2020. “A European Proficiency Test on Thin-film Tandem Photovoltaic Devices”. Loughborough University. https://hdl.handle.net/2134/13251119.v1.

Received: 5 March 2020 | Revised: 29 June 2020 | Accepted: 22 July 2020

DOI: 10.1002/pip.3322

RESEARCH ARTICLE

PROGRESS IN PHOTOVOLTAICS WILEY

A European proficiency test on thin-film tandem photovoltaic devices

Elena Salis[1] | Andreas Gerber[2] | Jens Wenzel Andreasen[3] | Suren A. Gevorgyan[3] | Tom Betts[4] | Blagovest Mihaylov[4] | Ralph Gottschalg[4] | Alp Osman Kodolbaş[5] | Okan Yilmaz[5] | Roman Leidl[6] | Marcus Rennhofer[6] | Shokufeh Zamini[6] | Maurizio Acciarri[7] | Simona Binetti[7] | Erwin Lotter[8] | Klaas Bakker[9] | Jan Kroon[9] | Wim Soppe[9] | Guillaume Razongles[10] | Lucia V. Mercaldo[11] | Francesco Roca[11] | Antonio Romano[11] | Jochen Hohl-Ebinger[12] | Wilhelm Warta[12] | José L. Balenzategui[13] | Juan F. Trigo[13] | Sebastian Neubert[14] | Diego Pavanello[1] | Harald Müllejans[1] | Iver Lauermann[14]

[1]European Commission, Joint Research Centre (JRC), Ispra, Italy

[2]IEK5–Forschungszentrum Jülich, Jülich, Germany

[3]Department of Energy Conversion and Storage, Technical University of Denmark (DTU), Roskilde, Denmark

[4]Centre for Renewable Energy Systems Technology (CREST), Loughborough University, Loughborough, UK

[5]Materials Institute, TÜBİTAK Marmara Research Center, Kocaeli, Turkey

[6]Austrian Institute of Technology (AIT), Vienna, Austria

[7]Solar Energy Research Center (MIB-SOLAR), University of Milano-Bicocca (UNIMIB), Milan, Italy

[8]Center for Solar Energy and Hydrogen Research Baden-Württemberg (ZSW), Stuttgart, Germany

[9]The Netherlands Organization for Applied Scientific Research (TNO), Petten, The Netherlands

[10]Commissariat à l'Energie Atomique Aux Energies Alternatives (CEA-INES), Le Bourget-du-Lac, France

[11]Italian National Agency for New Technologies, Energy and Sustainable Economic Development (ENEA) - Portici Research Centre, Portici, Italy

[12]Fraunhofer Institute for Solar Energy Systems ISE, Freiburg, Germany

[13]Centro de Investigaciones Energeticas Medioambientales y Tecnologicas (CIEMAT), Madrid, Spain

[14]PVcomB, Helmholtz-Zentrum Berlin für Materialien und Energie GmbH (HZB), Berlin, Germany

Correspondence
Elena Salis, European Commission, Joint Research Centre, Directorate C - Energy, Transport and Climate, Unit C2 - Energy Efficiency and Renewables, European Solar Test Installation (ESTI), via E. Fermi 2749 I-21027 Ispra (VA), Italy.
Email: elena.salis@ec.europa.eu

Present address:
Ralph Gottschalg, Fraunhofer Center for Silicon Photovoltaics (CSP), Halle, Germany; Faculty of Electrical Engineering, Manufacturing and Economic Engineering (EMW), Hochschule Anhalt, Köthen, Germany

Abstract

A round-robin proficiency test (RR PT) on thin-film multi-junction (MJ) photovoltaic (PV) cells was run between 13 laboratories within the European project CHEETAH. Five encapsulated PV cells were circulated to participants for being tested at Standard Test Conditions (STC). Three cells were a-Si/μc-Si tandem PV devices, each of which had a different short-circuit current ratio between the top junction and the bottom one; the remaining two cells were single-junction PV devices made with material representative of the individual junctions in the MJ cells. The RR PT's main purpose was to assess the capability of the participating laboratories, in terms of employed facilities and procedures, to test MJ PV devices. Therefore, participants

This is an open access article under the terms of the Creative Commons Attribution License, which permits use, distribution and reproduction in any medium, provided the original work is properly cited.
© 2020 European Union. *Progress in Photovoltaics: Research and Applications* published by John Wiley & Sons Ltd.

Funding information
European Union Seventh Framework Programme, Grant/Award Number: 609788

were requested to perform STC measurements of all cells according to their own procedure, which might not include external quantum efficiency measurements. The European Solar Test Installation (ESTI) of the Joint Research Centre (JRC) provided the reference calibrations against which the participants' results are compared. ESTI made also a verification of the cells performance at STC at the end of the RR PT, in order to allow a comparison between the initial stable state at which the cells were calibrated (just before circulation) and the one they had reached at the end of the RR PT. The overall results of the RR PT are here presented and discussed together with some aspects of MJ PV testing that emerged as not adequately applied or largely missing. Their full implementation is expected to improve the consistency of future results.

KEYWORDS
amorphous/micromorphous silicon, interlaboratory comparison, round-robin proficiency test, STC characterisation, tandem a-Si/μc-Si, thin-film multi-junction PV solar cell

1 | INTRODUCTION

Characterisation of photovoltaic (PV) devices has expanded since some years also to study their performance under working conditions that represent the ones PV modules meet in real installations more accurately than Standard Test Conditions (STC). A milestone in this process has been achieved with the series of international standards on the energy rating of PV modules,[1] which was completed in August 2018 with the publication of the last two parts of the series.[2,3]

Still, testing PV devices at STC remains important in order to set a reference point (i) to compare different PV technologies under the same reference testing conditions, (ii) to evaluate different modules of the same technology (e.g., crystalline Si) as produced by various manufacturers and (iii) as prerequisite to assess the variation in PV module and PV technology performance with change of operating conditions.[2]

Testing and calibration of single-junction (SJ) PV devices usually follows the broadly applied procedures of the standard IEC 60904-1,[4] with support of other standards by the International Electrotechnical Commission (IEC).[5–8] The latter are necessary in order to adjust the measurement conditions to STC or to correct the measurement results to values that have to be reported at STC. In particular, the measurement of the spectral responsivity (SR) according to IEC 60904-8[7] and the calculation of the spectral mismatch (SMM) according to IEC 60904-7[6] are crucial steps for reliable testing and calibration of any PV technology. This is valid in general for all measurement procedures, regardless of whether the correction for the SMM is applied *a posteriori* analytically or, on the contrary, made *a priori* by adjusting the solar simulator's irradiance before the current–voltage (I–V) measurement. The latter is indeed also a correction for SMM, achieved by using a reference device to set the effective irradiance as per IEC 60904-7.[6] This procedure in turn involves the SR of the reference device and of the device under test (DUT), the solar simulator's spectral and total irradiances and the reference spectrum[9] in the same way they are required for the *a posteriori* correction.

In the case of monolithic multi-junction (MJ) PV devices, the measurement procedure is more complex than for SJ, due to the intrinsically complex nature of MJ PV devices.[10] Monolithic MJ PV (from now on named only MJ PV) cells are made by two or more PV junctions that are mechanically and electrically connected in series in one single stack, accessible only through two terminals. Thus, the individual PV junctions cannot be directly accessed with non-destructive methods for electrical measurements. This constraint led to the development of more complex procedures to probe optical and electrical characteristics of MJ PV devices in order to test and calibrate them in a reliable way.

Although quite a recent introduction in the international standardisation of PV, testing of non-concentrating MJ PV devices is subject of two IEC standards that were published together in May 2017. The IEC 60904-1-1[11] deals with the measurement of the I–V characteristics of a MJ PV device. The IEC 60904-8-1[12] sets the requirements for their SR measurement, which involves on the one hand the use of specific bias light to activate the junction(s) not under test significantly more than the junction to be tested and, on the other hand, the use of a bias voltage to bring and keep the junction under test to short-circuit current conditions.

While the measurement procedures for most SJ PV devices were already well established and systematically applied in many laboratories, with a large variety of expertise levels and available facilities, MJ PV testing was still not fully integrated in the procedures of all laboratories at the time of the organisation of the measurement comparison reported here. This was also partly due to the lack of an internationally agreed standardised procedure to test them, although pre-normative research had already produced scientific publications on the topic (see, e.g., other studies[13–15]). In addition, as good practice for measurement and testing laboratories, and even required for

calibration laboratories accredited to ISO/IEC 17025,[16] in the last 30 years several interlaboratory comparisons and round-robins have already been organised for SJ PV testing at STC.[17–25] The World Photovoltaic Scale (WPVS) itself, which nowadays has become a sort of alias to refer to a solar cell with some standardised package, was in fact established in 1999 as measurement scale for PV starting from a dedicated world-wide intercomparison on calibration of PV cells.[26–28] Similar measurement comparisons are less numerous and less geographically wide in the case of MJ PV devices.[21,29–31] Also, a large part of those available is mainly related to concentrated PV (with reference to a total irradiance larger than 1000 W/m^2).[29–31]

Due to the limited number of measurement comparisons specific for terrestrial non-concentrating MJ PV devices, a first round-robin (RR) test on thin-film MJ PV cells was organised within the FP7 infrastructure SOPHIA project.[32] However, the test could not be completed due to technical issues with the circulated samples, which were not encapsulated and thus easily subject to mechanical damage.

Within the European FP7 project CHEETAH,[33] a second RR on thin-film MJ (tandem) PV cells was organised between 13 testing laboratories, which partly differed from the participants to the SOPHIA testing. The RR was organised as much as possible in the form of a proficiency test (***PT***), taking the ISO/IEC 17043[34] as guideline especially to assess the measurement results. The European Solar Test Installation (ESTI) of the Joint Research Centre (JRC), as laboratory accredited to ISO/IEC 17025 for SJ and MJ PV calibration,[35] provided the reference measurements of the RR PT (***RMPT***). ESTI was also in charge of the RR PT overall data analysis.

The main purpose of this second RR PT was to assess the capability of the participating laboratories in terms of their testing facilities and measurement procedures specific for MJ PV devices. For the participant laboratories, the technical competence of the personnel and the traceability to SI units were not evaluated separately from the assessment of the testing facilities and procedures, contrary to what usually happens in interlaboratory comparisons between testing and/or calibration laboratories that are all accredited to ISO/IEC 17025. The reference laboratory of the RR PT, instead, is required by ISO/IEC 17043 to have and prove adequate level of competence of the personnel involved in the PT measurements as well as unbroken traceability chain to SI units for the measurements performed. ESTI carries all this via its accreditation to ISO/IEC 17025 as mentioned above.

The evaluation of the laboratories' capability was carried out by comparing their measurement results against ESTI RMPT values. All 13 participants as well as ESTI used indoor procedures involving solar simulators to measure the circulated devices. Only one laboratory cross-checked the short-circuit current measured indoor with the value measured under natural sunlight. Preliminary results were presented at the EU PVSEC 2019,[36] where RR PT organisational aspects still to be improved were also discussed. In this paper, we aim at discussing in more detail all the RR PT results, not only in terms of comparison of the participants' submitted values towards ESTI calibration, but also highlighting the main sources that could explain some of the largest deviations and that can originate from missing steps in the testing procedure.

2 | METHODOLOGY

2.1 | Devices

Five PV devices were tested in the RR PT reported here. Among them, three were monolithic double-junction (or tandem) PV cells made of amorphous silicon (a-Si) deposited on top of micro-crystalline silicon (μc-Si). The other two devices were SJ PV cells made of a-Si and μc-Si, respectively. The inclusion of SJ cells in this RR PT on tandem PV devices was driven by the fact that even testing thin-film SJ cells involves expertise and specific steps in the measurement procedure that may not be correctly or completely available at all laboratories. The additional request to test separately also SJ PV cells of the same technology as those composing the tandem cells seemed quite reasonable in this RR PT, because checking the participants' capabilities in testing thin-film PV technologies was one of the targets of the RR PT.

Regarding the three tandem cells, they were prepared in such a way as to have a different ratio (i.e., balance) of the short-circuit current of the top junction as compared to the bottom junction. As well known, every series-connected PV device is limited by the current produced by the cell that less effectively responds to the actual operating conditions. From this point of view, a MJ PV device can be looked at as a special series-connected PV device, where one half of the cells (in the case of two junction types) is built and electrically contacted on top of the other half. However, contrary to series-connected SJ PV, in a MJ PV device the SR representative of one junction type is usually quite different from the other(s), with the result that the electrical limitation of the device is attributed generically to one of the junctions (called the *limiting junction*) rather than to a single cell. A currents' ratio or balance (CB) can then be calculated,[11] conventionally taking the junctions in the order in which they see the incoming light (i.e., top towards bottom). Usually, this ratio is referred to STC in order to set the reference conditions in the same way it is done for the electrical performance of the DUT. When the top junction is the limiting one, the CB value is smaller than 1. On the contrary, when the bottom junction is limiting, the CB value is larger than 1. In the case both junctions (ideally) deliver the same current, the ratio equals 1, and the PV device is defined *matched*. Of the three tandem cells included in this RR PT, one was identified by the producer as top-limited, one was nominally bottom-limited and the third was nominally matched. Table 1 lists the five PV cells together with the PV technology and the nominal junctions balance (where applicable) that characterise them. ESTI codes are used to identify them.

Each cell had a nominal active area of 1×1 cm^2 and was mounted in a metallic robust case under a glass window of about 3×3 cm^2, to ensure the mechanical protection of the cell during both transportation and testing (Figure 1). In particular, the case was provided with standard LEMO connectors (see Figure 1A) to make the connection operations easier and safer than with bare cells (used in the previous RR). The four-wire connection configuration (Kelvin probe) was used for them. Moreover, the solid-metal case assured good thermal conductivity between the cell and the external surface,

TABLE 1 List of the measured DUTs, including for each of them the PV technology and the device limitation (where applicable) as declared by the manufacturer

Device ID	PV technology of the solar cell	Nominal junction limitation
RR81	Amorphous silicon (a-Si)	Not applicable
RR82	Micro-crystalline silicon (μc-Si)	Not applicable
RR83	Tandem (a-Si/μc-Si)	Nominally top-junction limited
RR84	Tandem (a-Si/μc-Si)	Nominally bottom-junction limited
RR85	Tandem (a-Si/μc-Si)	Nominally matched

Note: For the junction-limitation certified by ESTI, see Table S1 in the supporting information.
Abbreviation: PV, photovoltaic.

facilitating its temperature control during I–V and SR measurements. A Pt100 temperature sensor was also integrated inside the case close to the solar cell and was connected to the outside via a LEMO connector. In order to avoid misconnections, the LEMOs were labelled PV for the cell and RTD for the Pt100 (see Figure 1A). Some connecting cables and adapters to banana connectors were provided as well, in order to improve the reproducibility of the measurements and broaden the connection options for the participants.

The five PV cells were made by Jülich Research Centre according to previously published procedures.[37,38] An initial pre-conditioning of the cells by light-soaking for 300 kWh in open circuit and at device temperature of 50° C was made at Jülich prior to the shipping to ESTI. However, as part of the standard procedure for thin-film PV device calibration at ESTI, all five cells were light-soaked once more at ESTI according to the IEC 61646 requirements[39] before the reference measurements (see Section 2.4.2).

2.2 | Organisation and protocol of the RR PT

As mentioned above, the purpose of the RR PT was to evaluate the capability of the participating laboratories in testing thin-film MJ PV cells (described in Section 2.1) by using their procedures and facilities. As the IEC standards for MJ PV devices[11,12] were not yet published at the beginning of the RR (although under advanced stage in the approval process[40,41]), the RR also aimed at collecting information about the possible improvements to be adopted in the measurement procedures as applied to MJ PV devices by laboratories active in European projects.

The RR was organised within the CHEETAH project[33] as a PT for 13 participating laboratories, also building on a failure analysis of the SOPHIA project's RR and on prior experience in interlaboratory comparisons.[21–23,25] The reference measurements were independently provided by ESTI, which calibrated all devices at the beginning of the PT (see Section 2.4). The devices were again shipped to ESTI at the end of the RR PT for a final verification and calibration. The standard ISO/IEC 17043[34] was taken as guideline for the evaluation of the participants' results, as already done in previous similar exercises for PV.[23,25]

As initiator of the RR within the CHEETAH project, Helmholtz-Zentrum Berlin (HZB) acted as the coordinator (but not as the official provider in the sense of ISO/IEC 17043[34]) of the RR PT, although it was also a PT participant. This double role of one participant is usually avoided in PTs organised by official PT providers for testing laboratories, in order to assure unbiased results assessment. However, two elements allowed considering HZB position not detrimental to the good development of this specific RR. First, HZB's double role had been taken into account within the CHEETAH project, with no objection by any participant. Second, although the participants' results were submitted to both the coordinator and ESTI, the data analysis of the overall RR PT was made by ESTI, with no disclosure of the RMPT calibration value before the end of the project.

A guideline was circulated to the participants before the beginning of the RR, with instructions on how to handle the DUTs and which type of information was needed in order to compare each participant's results to the RMPT values by ESTI. The participants were required to test each DUT at STC according to their standard procedure for the specific type of DUT. In particular, they were asked to apply their usual procedure for testing MJ PV devices, with possibly incomplete or incorrect steps in the specific applied procedure. However, identifying such insufficiencies was also part of the study, allowing a realistic verification of the capability of the participants in terms of facilities and procedures and the identification of possible areas for measurement improvements and best practices sharing.

In addition, as not all laboratories could perform an adequate preconditioning of the PV cells before testing them, it was agreed that all participants should measure the DUTs without further stabilisation (other than the one performed at ESTI before the reference calibration). This could affect the measurements at successive laboratories if changes related to metastability of the devices occurred, but at the time of the RR organisation it was considered a balanced approach to verify the measurement procedures at the laboratories without affecting the duration (and the cost) of the overall RR PT. To monitor possible exposure to high temperatures during the shipments, which might alter the stabilisation state of the a-Si based PV cells, the devices were provided with irreversible thermal-sensitive labels attached to their case (see Figure 1B) in Section 2.1), and the participants were asked for reporting any indication of heat excess. No mechanical monitoring was used to identify mechanical shocks during transportation, because the latter was considered a less likely threat for these robustly encapsulated thin-film cells.

In general, the procedure to attain STC for I–V measurement can be done either *a priori*, by adjusting both intensity and spectrum of the solar simulator with a spectrally-matched reference cell (RC) (in this case, necessary for all types of DUTs regardless of the number of junctions), or *a posteriori*, by applying the SMM correction,[6] which in the case of MJ PV has to be the one calculated for the limiting junction (defined in Section 2.1). In the case of an *a posteriori* correction, the SMM had to be submitted, too. It was also requested to

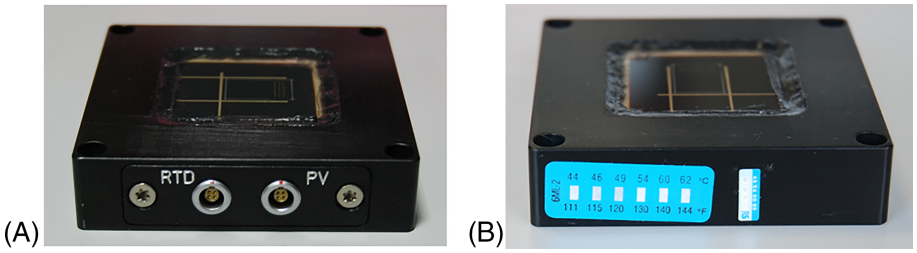


FIGURE 1 One example of the encapsulated PV solar cells, with connectors for temperature (RTD) and electrical (PV) characterisation (A) and thermal-sensitive labels (B) [Colour figure can be viewed at wileyonlinelibrary.com]

indicate which junction was found limiting for the tandem cells. Beside I–V curve measurements, SR data were required in the case SR measurement was part of the laboratory's procedure. For the MJ PV cells, the information to be submitted for SR measurements included the bias voltage applied to the DUT as well as the bias light spectrum. Finally, all the four main I–V parameters, namely, short-circuit current I_{SC}, open-circuit voltage V_{OC}, maximum power P_{max} and fill factor *FF* had to be reported together with a measurement uncertainty (UC) estimate.

The guideline included also a description of the devices to be measured (see Section 2.1) with their nominal characteristics as assigned by the producer. In this way, a suitable voltage limitation could be used during the I–V measurements in order to avoid damaging the thin-film cells by reverse overcurrent.

2.3 | Participants

The laboratories participating in the RR PT were 13 (see Appendix A). Each of them had its own facilities and expertise to test MJ PV devices. All of them used a solar simulator to measure the I–V curves. Some of them did not adjust the solar simulator other than for total irradiance as read by a c-Si RC. Three quarters of the laboratories measured the external quantum efficiency (EQE) (or the SR) of the DUTs, but only very few of them corrected spectral deviations from STC in the I–V measurements by considering the measured actual SR of the DUT. Finally, about only one third of those who measured EQE applied a bias voltage to the EQE measurement of the MJ PV DUTs. A more detailed summary of the facilities and procedures available at the time of the RR PT is given for each participant in Appendix A.

2.4 | ESTI measurements

Before the start of the RR, the STC calibration of the five cells was performed at ESTI in January 2016. These five calibrations were the ***reference measurements of the RR PT*** (RMPT); against their values, the results submitted by every participant to the RR PT were compared. A verification at the end of the RR was also made at ESTI in the form of a calibration, although those measurements were not used to assign the RMPT value but just to verify the actual stability of the devices. Indeed, reliable measurements, repeated at the same laboratory at least at the beginning and at the end of a RR, can help explaining possible deviations of the participants' results if related only to their positioning within the temporal sequence of the RR PT.

2.4.1 | ESTI setups

ESTI used a Wacom steady-state solar simulator[42] for the I–V measurement of the cells. The RC used for the DUTs was an unfiltered c-Si calibrated RC (ESTI code: PX305C), except for RR81 for which a filtered c-Si calibrated RC was used (ESTI code: PX301A). Both RCs are secondary references at ESTI, under the meaning of the traceability chain, and traceable to the WPVS.[28] Their absolute SR is shown in Figure 2. The vertical positioning of the temperature-controlled plate used to thermalise the devices was adjusted in relation to the device mounted (RC or DUT) to maintain the same test plane for both. The ESTI procedure to measure I–V curves at the Wacom requires keeping its shutter closed in order to allow for stabilisation of the DUT's temperature. When the latter is achieved, the shutter is opened to illuminate the DUT for 3 to 5 seconds before the I–V curve (made of 100 points) is acquired in 1 s.

For the SR of the five DUTs, the ESTI's semi-automatic home-built setup named Oriel (after the solar simulator providing the light source) was used.[43] In short, the white light of its Xenon source is filtered by interferential bandpass filters (typical FWHM between 10 nm and 20 nm) and reaches the DUT and the RC after passing a chopper and an optics that ensure that both devices are fully over-illuminated. The wavelength associated to each filter is periodically

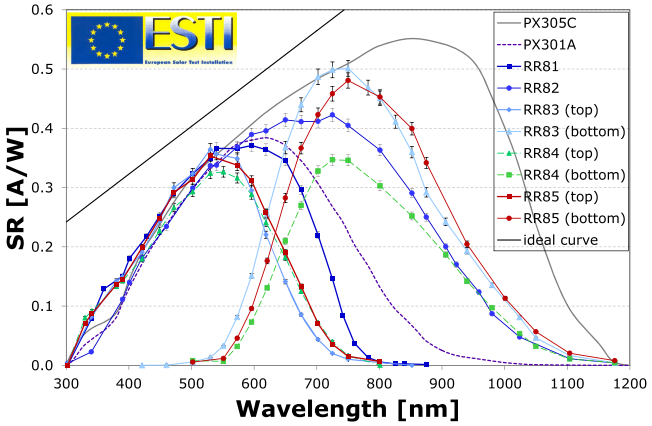


FIGURE 2 Absolute SR data of the five PV DUTs as certified by ESTI calibration at the beginning of the RR PT. The error bar drawn for each measured point represents its stated combined expanded UC (k = 2) in absolute units. Lines drawn to connect the individual measured points of the DUT SRs are merely shown to help the reader's eye and do not represent neither measured data nor actual interpolation between them. The interpolated SR of the RCs (PX305C and PX301A) used to calibrate them is shown, too. [Colour figure can be viewed at wileyonlinelibrary.com]

verified at ESTI by a double-beam spectrophotometer. The wavelength calculated from the measured transmissivity is used as the actual abscissa value for the SR data point. The filters are mounted on several wheels, each of which hosts 16 positions. Depending on the PV device and technology to measure, two or more wheels are mounted in the setup sequentially, and the signal corresponding to each wavelength is measured by a lock-in technique for both DUT and RC simultaneously. While the SR measurement proceeds, each measured data point is added to the SR graph shown to the operator on the screen. In this way, an immediate qualitative check can be made and the operator can select the more appropriate filters to fill the gaps in the SR curve, especially where steep features occur. The wavelengths are always selected to adequately cover the entire wavelength range of the DUT's SR as well as to allow an appropriate interpolation (with 1-nm step) of the measured data points by Hermite polynomial; the interpolated data set is then used for further calculations, e.g. for the SMM estimate. For SJ PV cells, broadband dichroic halogen lamps were used as bias light. For the three MJ PV cells, a pair of LEDs was used to bias the junction not under test, and a power supply was used to apply the bias voltage. More detailed description of the setup and measurement procedure is given in Section 2.4.3.

2.4.2 | Pre-conditioning before calibration

Before the actual calibration measurements, the cells went through the ESTI procedure for their pre-conditioning, which was carried out according to IEC 61646[39] between December 2015 and January 2016. Such a procedure is based on international standards developed at the IEC. In particular, at the time of the start of the RR, the standard IEC 61646[39] for design qualification of thin-film PV technologies was in place and therefore applied before the RMPT. As first step, STC measurements at the Wacom steady-state solar simulator of ESTI were performed to set the initial state of each DUT. Although it was not required by the pre-conditioning procedure according to IEC 61646,[39] the SR before the pre-conditioning was measured as well in order to (i) calculate the SMM to be applied to the I–V measurements, (ii) identify the limiting junction of the tandem DUTs before pre-conditioning and (iii) verify if any change to the limiting junction could occur due to the light-soaking procedure. Each DUT was then connected to a resistor, which was sized to keep the DUT approximately at the maximum power point as calculated from the initial I–V curves. The DUTs were finally mounted on a dedicated holding structure and put in a ventilated light-soaking chamber for a total of about 234 kWh, divided in three steps. The temperature of each DUT was constantly monitored by a calibrated Pt100 sensor attached to the DUT case and connected to a calibrated temperature reader. The temperature was maintained at (45 ± 5) °C for the whole pre-conditioning. The first pre-conditioning step had to be particularly long (about 133 kWh) due to temporary unavailability of the Wacom solar simulator. The second and the third lasted about 50 kWh each. At the end of each light-soaking step, the five DUTs were disconnected from their load, tested at STC at the same solar simulator and with the same RC as in the initial measurements and finally repositioned in the light-soaking chamber to continue the pre-conditioning. As these intermediate measurements are only relative measurements and the Wacom irradiance is known to be stable from periodic characterisation, no SMM correction was applied to them, and the criterion for stability check[39] was verified by comparing the maximum power values as calculated directly from the measured I–V curves.

For the sake of completeness and guidance to the reader, it is worthy to note that the CB value for a MJ DUT can generally be expected to change whenever the SRs of the junctions of which it's composed change relatively to each other during the pre-conditioning. However, the relevance of this possibility and the need for its verification should always be evaluated in relation to the purpose of the measurements to be performed. On the basis of the SR measurements made by ESTI and of the spectra of the Wacom solar simulator, all measured before and after the pre-conditioning of the DUTs, the calculated CB values showed changes due to pre-conditioning in a range from about −14.6% to about 7.5%, depending on the DUT and on the spectrum (i.e., AM1.5 or Wacom's) considered. The summary of the CB values and the relevant information used to calculate them is reported in Table S2 of the supporting information together with the Z_i factor defined in IEC 60904-1-1.[11] The absolute SR of the stable DUTs is shown in Figure 2; the normalised EQEs of the DUTs calculated from ESTI SR measurements before and after the pre-conditioning are reported in Section 3.2 (Figures 8, 9 and 10), which is specifically dedicated to the SR results of the RR PT. The two spectra of the Wacom and the AM1.5 reference spectrum are shown in Figure S1 of the supporting information. Finally, it must be noted that no attempt was made to improve the balance of the Wacom's spectrum beyond what was already its status in the case of the measurements before the pre-conditioning, as the I–V measurements on the as-received DUTs were just used for stabilisation purposes and ESTI did not issue any calibration certificate on the basis of those measurement results.

2.4.3 | Reference measurements of the RR PT

Once the DUTs were deemed electrically stable, their calibration at STC was performed. The latter was based on I–V curve measurements carried out at the Wacom solar simulator against a calibrated WPVS-traceable c-Si RC (ESTI code: PX305C) for all devices but the a-Si RR81, for which a calibrated WPVS-traceable filtered c-Si RC (ESTI code: PX301A) matched to the DUT was used.

Each device was mounted in turn on a Peltier temperature-controlled plate to keep it thermally stable at (25.0 ± 0.5) °C. The device was let stabilise with the plate and in the dark before proceeding with the measurements. As no traceability to SI units could be assured by ESTI for the internal temperature sensor of the RR cells, the device temperature was measured by a calibrated Pt100 sensor attached to the side of the case and as close as possible to the cell. The Pt100 sensor was in turn connected to a calibrated temperature

reader, whose reading was recorded together with the electrical characteristics of the DUT. The inevitable small but not negligible temperature rise after the DUT exposure to irradiance and the temperature gradient between the measurement point and the junction are included in the combined expanded UC (k = 2) stated with the ESTI calibration value of each DUT.

The total irradiance was set beforehand to be as close as possible to 1000 W/m^2, with a deviation of −4 W/m^2 for all DUTs but the a-Si one, for which a maximum deviation of −25 W/m^2 was achieved, as measured by the relevant calibrated RC before and after the I–V measurements. The spectral content of the Wacom's beam between [300; 2500] nm is periodically checked at ESTI by a traceably calibrated spectroradiometer and, if necessary, readjusted to AM1.5 by balancing the component beams produced by its double-lamp system. However, in the case of this RR PT, the spectral irradiance measurement was also specifically performed in the limited wavelength range [300; 1200] nm by means of the calibrated spectroradiometer (OL750, traceable to SI units via a calibrated standard FEL lamp, which is traceable via the UK's National Physical Laboratory (NPL)) immediately before the calibration of the cells.

In order to complete the set of measurements necessary for the calibration of the five DUTs, a SR measurement was performed for each of them according to the specific ESTI procedures, which make use of the lock-in technique. ESTI procedures follow the relevant standard for SJ SR[7] or MJ SR[12] measurements, depending on the case. In particular, although the IEC 60904-8-1 was not yet published at the beginning of this PT, ESTI procedure was covered by the laboratory's ISO/IEC 17025 accreditation; also, it already reflected one of those now included in the IEC 60904-8-1, because ESTI contributed pre-normative work to the standard and led the development of both IEC standards for testing of MJ PV devices.

The SR of the SJ DUTs was measured against a calibrated c-Si RC (ESTI code: PX302C, whose absolute SR is traceable via PTB) by applying white bias light produced by halogen lamps and no bias voltage.[43] The SR of the double-junction DUTs was measured at the same facility and against the same RC, but by applying bias light from two pairs of LEDs with emission lines around 860 nm to measure the top junction (i.e., bottom-junction activation) and around 410 nm to measure the bottom junction (i.e., top-junction activation). A specific level of bias voltage, necessary to bring and keep the junction under test to short-circuit current conditions during SR measurement of MJ PV,[12] was applied to each junction of each MJ DUT. According to ESTI procedure, the value of the bias voltage was determined for each junction of each tandem DUT separately. First, the voltage at the terminals of the electric circuit consisting of the DUT plus a dedicated stable power supply (set initially at 0 V) was measured with a calibrated digital voltmeter. This voltage measurement was carried out while the DUT was kept under bias-light condition only (i.e., no AC component from the chopped quasi-monochromatic light of the SR system). In general, such a voltage accounts for the actual voltage as produced by the junction(s) not under test, plus an insignificant contribution due to the actual connections involved. The voltage measured in this way was then brought to zero by adjusting the output of the power supply, while keeping the latter connected to the DUT and the voltmeter. Once the balance condition between the voltage from the DUT and the opposite one from the power supply was achieved, the two terminals of the above-mentioned electric circuit were disconnected from the voltmeter and connected to a calibrated precision shunt across which the DC + AC signal was then measured. A final check was made by connecting the voltmeter in parallel to the precision shunt in order to verify that the voltage drop across the shunt itself was less than 3% of the initial voltage as previously measured under bias light conditions only. For all SR measurements, the DUTs as well as the RC were mounted on a dedicated temperature-controlled plate in order to keep them at (25.0 ± 1.0) °C. The absolute SR data used for the RMPT calibration are shown in Figure 2 for all five DUTs. The error bar drawn for each measured point represents its stated UC in absolute units. Lines drawn to connect the individual measured points of the DUT SRs are merely shown to help the reader's eye and do not represent neither measured data nor actual interpolation between them. Interpolated SR curves of the unfiltered (PX305C) and filtered (PX301A) c-Si RCs used to calibrate the DUTs are shown as well, in order to give a visual comparison of the difference between the RCs and the DUTs.

The calibration of each DUT was then completed by correcting the measured I–V curves with the relevant SMM. In the case of a MJ DUT, the SMM calculated for the limiting junction was applied to correct the I–V curves and issue the calibration value. Correction for series resistance was not performed, as the I–V measurements were made at (25.0 ± 0.5) °C and at 1000 W/m^2 ± 30 W/m^2, which at ESTI is taken as boundary for mandatory correction for series resistance on the basis of experience. The calibration results, which represent the RMPT values for each device, are summarised in Table S1 (in the supporting information) together with the SMM applied to the measured I–V curves and the limiting junction for each of the tandem cells. One example of the measured I–V curves for each DUT is also shown in Figure S2. The curves reported in Figure S2 are those as measured directly on the solar simulator and corrected to a total irradiance of 1000 W/m^2 according to IEC 60891.[5] There is no correction point-by-point for irradiance fluctuations of the data in the I–V curve, because the solar simulator has a stabilised output (using an optical sensor and electrical feedback circuit). The variation of total irradiance between its measurement by the RC just before the I–V curve acquisition and its values during the actual I–V curve is considered as an UC component, which however gives a minor contribution to the expanded combined UC (k = 2).

For the sake of completeness, it has to be noted that the SR of the μc-Si device (RR82) is significantly different from both the one that the μc-Si bottom junction presents inside the tandem DUT and the one of an unfiltered c-Si RC, as clearly visible in Figure 2. The major difference with the bottom junction of the tandem DUT is due to the filtering effect that the top junction of the tandem devices has on the incoming irradiance. Consequently, one cannot assume that the μc-Si bottom junction has a SR similar to the SJ μc-Si device and a specific spectral correction has to be made in order to correctly calibrate the MJ PV device that includes a μc-Si junction. The same is valid when testing the SJ μc-Si device against a c-Si RC.

2.4.4 | Verification and calibration at the end of the RR PT

At the end of the RR PT, the cells were returned to ESTI for a final verification of their stability state (as they arrived) and for an additional calibration after a further pre-conditioning of 170 kWh. A full set of measurements was carried out as for the RMPT, except for the SR measurements before the new stabilisation, which were not performed. It was assumed that no significant change in the relative SR could have been introduced to the DUTs after the initial stabilisation and during the RR PT. Both sets of ESTI measurements performed at the end of the RR PT served mainly as comparative measurements with respect to the RMPT. The verification made when the cells returned to ESTI was considered useful to set a freshly and independently verified state of the DUTs, which for example could give additional information to explain part of the deviations from the RMPT value if a systematic trend were to be observed in the temporal sequence of the results. After the initial measurements, all five DUTs went through the same light-soaking procedure as explained in Section 2.4.2, with the exception that the standard IEC 61215-1-3[44] was used as reference instead of the IEC 61646. Indeed, in December 2016, the latter was withdrawn and replaced by most of the parts of the new IEC 61215 series[45]; in particular, a-Si PV devices are now subject of the IEC 61215-1-3.[44]

2.5 | Methodology for results assessment

As mentioned above, the methodology used to assess the participants' results against the reference value was based on the standard ISO/IEC 17043[34] and on previous experience.[21–23,25] The comparison of each result to the RMPT value was originally meant to be done by considering the UC of the measurements for each measurand, as stated by each laboratory according to its own method to estimate it. Ideally, the assessment of the PT results would be carried out by calculating—for each measurand and submitted value—one E_n number as defined in ISO/IEC 17043 and explained for example in freely accessible references.[23,25,46] However, this advanced methodology could not be applied to this RR PT due to the lack of any UC statement for 7 laboratories out of 13 participating, regardless of their level of expertise or quality of their facilities. Therefore, only simple percentage deviation from the RMPT value was calculated and is reported here for results as submitted by each laboratory.

3 | PT RESULTS AND DISCUSSION

3.1 | Electrical parameters assessment

For each laboratory and device, the percentage deviations in I_{SC}, V_{OC}, P_{max} and *FF* from the relevant RMPT value were calculated; they are reported in one graph per device in the following subsections. In the graphs, the UC of the RMPT value is shown as a shaded area symmetrically drawn around the *x*-axis. The RMPT's UC is shown only for P_{max} (light-grey area) and *FF* (dark-grey area) to limit the complexity of the graphs while preserving the relevant information. Indeed, in the graph, the area of the ESTI UC for I_{SC} would be slightly narrower than that of P_{max}, and the one for V_{OC} would almost disappear within the *x*-axis line.

In addition, also the measurement UC stated by each laboratory, when available, is reported for each measurand as error bar around the submitted value. In this way, for those who reported a measurement UC, a better representation of the agreement of their submitted value to the RMPT value is presented. In few P_{max} cases, the error bars are hidden by the size of the marker. However, these occurrences can be usually and easily spotted because the error bars of the other parameters are reported by the same laboratory. When the result's error bar does not overlap the UC bar of the corresponding RMPT value, the submitted result has to be carefully reconsidered together with its UC and measurement procedure. However, also UC bands slightly overlapping might be not enough, as only the actual calculation of the E_n number can assess whether a result agrees or not with the reference value within its stated UC.

As general rule applicable to this RR PT (where only some laboratories have submitted UC with their results), a full agreement to the RMPT value is obtained either when the submitted result is within the UC band of the RMPT value or when the E_n number that can be calculated with the UCs is within [−1; 1]. Considering the variety of expertise and facilities involved in this RR PT, in the assessment of the results, we have considered a deviation's threshold of ±5% as representing still a reasonable UC for the majority of the laboratories. A submitted result falling within this threshold would be considered still satisfactory in this RR PT, although it might be beneficial for the laboratory to revise the UC and/or the procedure to improve the agreement with the RMPT value. Any value outside of this threshold requires careful evaluation and revision of both the UC calculation and the measurement procedure, including the equipment.

To keep anonymity of the results, each laboratory is represented in the graphs by one number on the *x*-axis, which scales from 1 to 13. It has to be noted, though, that the number identifying one laboratory is not necessarily always the same for all five figures. Indeed, in order to ensure the highest level possible of anonymity, the ranking criterion chosen to sort the laboratories is given by the percentage deviation of the submitted P_{max} value from the RMPT value. Since such a deviation can vary for the same laboratory from DUT to DUT, it also makes the sorted list vary for each DUT. In fact, this is to be expected when no systematic errors affect the measurements of the participants. In addition, the sign of the deviations is explicitly considered. As consequence of all this, position 1 on the *x*-axis of each graph is assigned to the laboratory with the largest negative (or smallest positive) percentage deviation of P_{max} from the RMPT P_{max} value for that DUT; equally, position 13 is assigned to the largest positive (or smallest negative) percentage deviation from the RMPT P_{max} value for that DUT. The positions in between are assigned in order of increasing deviation.

3.1.1 | RR81 (a-Si SJ DUT)

Figure 3 shows the percentage deviations of the submitted results from the RMPT values for the DUT RR81 (a-Si). The EU and ES values correspond to the ESTI measurements made at the end of the RR PT before and after the pre-conditioning, respectively. The light-blue-shaded area helps in separating them from the results of the RR PT participants, too. Only three laboratories (#8, #9 and #10) out of 13 participants have submitted a result for P_{max}, considered together with its UC, that is within the UC of the RMPT value. If we set an arbitrary threshold at ±5% of the RMPT value, only two additional P_{max} values (#11 and #12) are within that threshold.

Among the remaining participants, the results of four laboratories (#1, #3, #5 and #6) were biased by an electrical issue occurred at #1, which affected the DUT and therefore the measurements of all the following participants to the PT. For these four laboratories, it is clearly visible that the large deviation in P_{max} is correlated to a similar large deviation in *FF*. Although *FF* is just a derived parameter, that is, calculated from a ratio of the measured maximum power to the ideal one, it is also strongly affected by bad electrical connections to the DUT and/or by bad collection of charges inside it. The I_{SC} and V_{OC} deviations, instead, are generally much smaller for all four and within −2.7% for the three laboratories following the accident. Therefore, it is reasonable to deduce that the agreement of their P_{max} results with the RMPT value could have been much better if the electrical issue had not occurred.

For the remaining four laboratories (i.e., #2, #4, #7 and #13), which were not affected by the mentioned electrical issue, the deviation in P_{max} is strongly connected to the deviation in I_{SC}, which is well

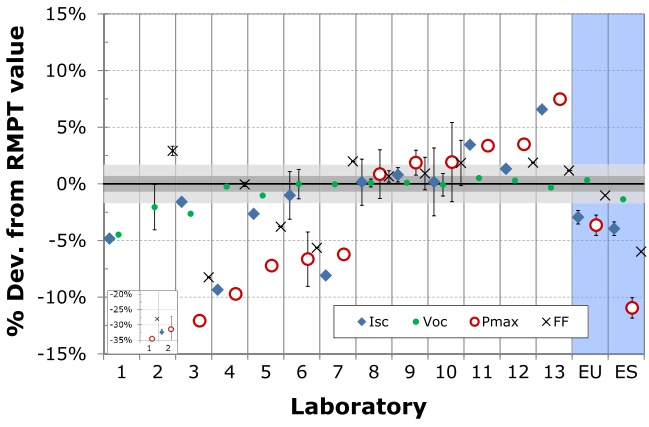


FIGURE 3 Percentage deviations from ESTI RMPT value for I_{SC}, V_{OC}, P_{max} and *FF* of RR81 (a-Si). RMPT value is represented by the *x*-axis, and its combined expanded UC (k = 2) is shown for simplicity only for P_{max} (light-grey-shaded area) and *FF* (dark-grey-shaded area). The error bars shown represent the UC of the submitted result as stated by the participant. The EU and ES values correspond to the ESTI measurements made, respectively, before and after the pre-conditioning at the end of the RR PT. An inset is shown for the points falling outside the main range of the deviations. Note that the laboratory identification number may be different for the DUTs [Colour figure can be viewed at wileyonlinelibrary.com]

beyond ±5% of the RMPT value. This is likely related to issues with SMM correction. They can originate from two sources. The first is the use of non-spectrally matched RC together with no or insufficient SMM correction (e.g., due to the test spectrum used to calculate SMM). The second is the incorrect or incomplete adjustment of the solar simulator spectrum, which in turn can be linked again to issues with the RC(s) used to adjust it. Laboratory #2 did not measure the EQE and did not adjust the spectral irradiance of the solar simulator used for the I–V curve measurements. Therefore, no spectral correction was applied neither a priori nor a posteriori. Laboratory #4 provided UCs, which are however so small that they are not visible in the graph. At this laboratory, there seems to be no issue neither with V_{OC} nor with *FF*, so the large deviation in P_{max} and I_{SC} is extremely likely to be due to SMM correction (either *a priori* or *a posteriori*) or incorrect calibration of the RC. Laboratories #7 and #13 corrected (either a priori or a posteriori) the I–V curve measurements for SMM, but it is clear that the procedure to achieve the SMM correction, the RC calibration value or a combination of these two did not lead to a satisfactory result.

Finally, for the sake of completeness, it has to be noted that no pre-conditioning of the DUT was done at the participants' premises because not everybody could do it. As a-Si is intrinsically unstable and the RR lasted more than 1 year, it could also be expected that the degradation of the a-Si stable state achieved at ESTI at the beginning of the RR partially affected the results of some of the last laboratories in the RR progression. A deviation of −3.6% in P_{max} from the RMPT value was measured at ESTI (EU in Figure 3) at the end of the RR, when the DUT returned there, and before any further pre-conditioning to take it back to a stabilised state. The additional stabilisation brought this DUT to a P_{max} value −10.9% (ES in Figure 3) smaller than the RMPT value, showing a significant change in the electrical performance of the device. However, the long-term degradation before any additional stabilisation (−3.6%), which also accounts for the mentioned electrical issue, cannot explain the deviation of the laboratories beyond the ±5% threshold (excluding those affected by the issue at laboratory #1), because laboratories #2, #4, #7 and #13 performed their measurements quite early in the RR. Thermal issues to the cells during the several shipments can also be excluded as possible source of the deviation of these laboratories, because the thermal sensitive labels attached to the cells were still unaltered when the DUTs arrived at laboratory #1. Therefore, a possible spectral issue should be investigated and a more complete UC analysis performed at laboratories #2, #4, #7 and #13.

3.1.2 | RR82 (µc-Si SJ DUT)

Figure 4 shows the results for RR82, which is the µc-Si DUT. The EU and ES values correspond to the ESTI measurements made at the end of the RR PT before and after the pre-conditioning, respectively. The light-blue-shaded area helps in separating them from the results of the RR PT participants, too. For four laboratories (from #4 to #7), the submitted value for P_{max} agrees with the RMPT value either within

their own UC (as for #4) or because the value itself, although submitted without UC, is within the UC band of the RMPT value (as for #7).

Among the other participants, seven out of 13 are beyond the RMPT UC for P_{max} but within the arbitrary threshold of ±5% of the RMPT value. Due to lack of UC information, no additional comment can be made except that the value submitted by laboratory #8 is 0.2% above the UC band of the RMPT value and that the submitted I_{SC} value is within the UC of the RMPT value (UC band not shown in the graph). Therefore, it is reasonable to assume that, including realistic UC for the submitted results, laboratory #8 would also agree with the RMPT value. The last two laboratories out of 13 are beyond ±5% but within ±10% of the RMPT value, and their stated UCs clearly show that the procedure and/or the UC estimate should be reanalysed. For most laboratories, though, there seems to be in general some inaccuracy or incompleteness in the spectral correction of the measurement (achieved either a priori or a posteriori) and/or in the calibration value of the RC(s) used to set the solar simulator. It is difficult to say for which laboratory this is fully valid and for which this is only a matter of missing UC information. However, apart from the four above-mentioned laboratories that agree with the RMPT value and for laboratory #8 whose I_{SC} leads to considering sensible a possible agreement if reasonable UC were provided, for all others the deviation of I_{SC} from the RMPT value is beyond ±3% and its causes should be carefully analysed by the individual participants.

The change in P_{max} measured at ESTI at the end of the RR PT was +3.9% (EU in Figure 4), which after further stabilisation went down to +0.5% (ES in Figure 4). The latter value is well within the UC of ESTI measurement. However, from the temporal sequence of the laboratories (not shown here), none of them submitted a deviation that can be explained by such a degradation in relation to their temporal positioning.

Finally, it is worthy to note here that this DUT has SR closest to the SR of a typical c-Si RC in comparison to all other DUTs (see RR82 in Figure 2). However, it would be wrong to assume that no SMM correction were needed, as SMM is a measurement of both how far the SR of the DUT is from that of the RC as well as how much the test spectrum differs from the reference AM1.5. This is evident for laboratory #1, which did not correct for spectral deviations from STC neither a priori nor a posteriori and whose measurement UCs are not sufficient to explain the deviation from the RMPT value for neither P_{max} nor I_{SC}.

3.1.3 | RR83 (a-Si/μc-Si MJ DUT)

Figure 5 reports the results for RR83, which was nominally labelled as the top-limited DUT (see Table 1) and certified by ESTI as such at the beginning of the RR (see CB in Table S2 in the supporting information). The EU and ES values correspond to the ESTI measurements made at the end of the RR PT before and after the pre-conditioning, respectively. The light-blue-shaded area helps in separating them from the results of the RR PT participants, too. Among the participants, only three laboratories (#4, #5 and #6) agree with the RMPT P_{max} value: the first two directly because they are within the UC band of the RMPT value; the third one because its UC almost intersects the RMPT value and the E_n number is 0.87, which represents agreement with the RMPT value (one can refer for example to open-access peer-reviewed references[23,25,46] for the E_n number calculation). The

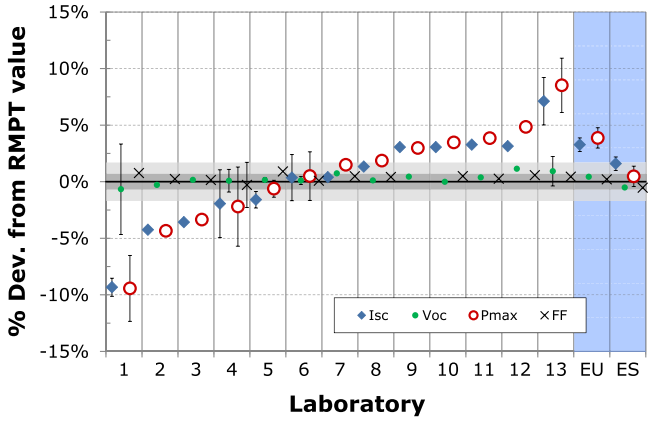


FIGURE 4 Percentage deviations from ESTI RMPT value for I_{SC}, V_{OC}, P_{max} and *FF* of RR82 (μc-Si). RMPT value is represented by the *x*-axis, and its combined expanded UC (k = 2) is shown for simplicity only for P_{max} (light-grey-shaded area) and *FF* (dark-grey-shaded area). The error bars shown represent the UC of the submitted result as stated by the participant. The EU and ES values correspond to the ESTI measurements made, respectively, before and after the pre-conditioning at the end of the RR PT. Note that the laboratory identification number may be different for the other DUTs [Colour figure can be viewed at wileyonlinelibrary.com]

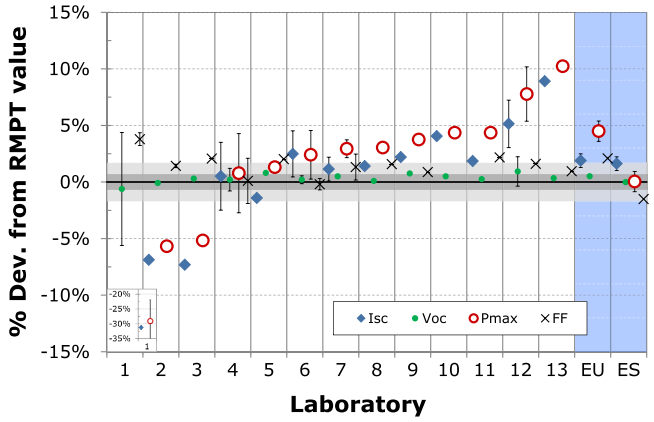


FIGURE 5 Percentage deviations from ESTI RMPT value for I_{SC}, V_{OC}, P_{max} and *FF* of RR83 (a-Si/μc-Si). RMPT value is represented by the *x*-axis, and its combined expanded UC (k = 2) is shown for simplicity only for P_{max} (light-grey-shaded area) and *FF* (dark-grey-shaded area). The error bars shown represent the UC of the submitted result as stated by the participant. The EU and ES values correspond to the ESTI measurements made, respectively, before and after the pre-conditioning at the end of the RR PT. An inset is shown for the points falling outside the main range of the deviations. Note that the laboratory identification number may be different for the other DUTs [Colour figure can be viewed at wileyonlinelibrary.com]

agreement in I_{SC} (for #5 because it is within the UC band of the RMPT value for I_{SC}) fully confirms this.

Of the other 10 participants, 5 (from #7 to #11) are within the arbitrary threshold of ±5% of the RMPT P_{max} value. If we analyse their deviation of I_{SC} in addition to the one for P_{max}, we find that both laboratories #7 and #8 have submitted I_{SC} values that deviate from the relevant RMPT value less than its UC. Therefore, they do agree for I_{SC} with it. While laboratory #8 did not submit any UC for P_{max}, laboratory #7 did submit a P_{max} UC that seems to be somehow underestimated. Within the same group of five laboratories, #9 and #11 might benefit from a reanalysis of the procedure for the (*a priori* or *a posteriori*) spectral correction because the deviation of their submitted value of I_{SC} is just above the UC band of the relevant RMPT value (0.6% and 0.3%, respectively). For the remaining laboratory (#10) of this group as well as (and especially) for those beyond the ±5% threshold, the results show the necessity to carefully reconsider their procedure for MJ testing, with clear evidence that the correction for spectral effects (either from the SR of the DUT or from the spectrum of the solar simulator) is not adequately performed.

The P_{max} change for this cell during the RR PT was of +4.5% (EU in Figure 5), which returned to +0.0% after the final stabilisation (ES in Figure 5). None of the laboratories that show deviations beyond ±5% can relate them to this because of their positioning in the RR PT temporal sequence.

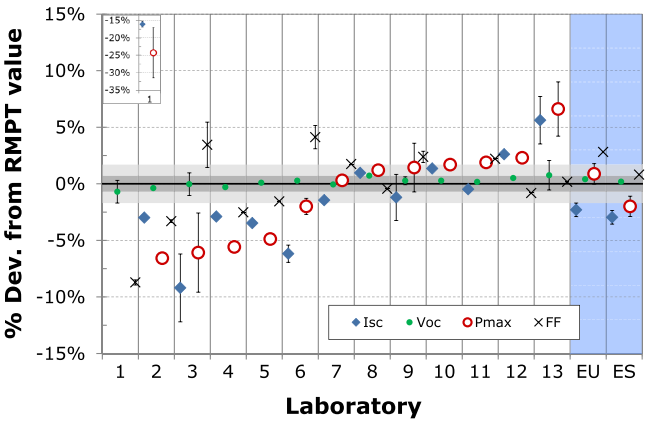


FIGURE 6 Percentage deviations from ESTI RMPT value for I_{SC}, V_{OC}, P_{max} and *FF* of RR84 (a-Si/µc-Si). RMPT value is represented by the *x*-axis, and its combined expanded UC (k = 2) is shown for simplicity only for P_{max} (light-grey-shaded area) and *FF* (dark-grey-shaded area). The error bars shown represent the UC of the submitted result as stated by the participant. An inset is shown for the points falling outside the main range of the deviations. The EU and ES values correspond to the ESTI measurements made, respectively, before and after the pre-conditioning at the end of the RR PT. Note that the laboratory identification number may be different for the other DUTs [Colour figure can be viewed at wileyonlinelibrary.com]

3.1.4 | RR84 (a-Si/µc-Si MJ DUT)

Figure 6 gives the results for RR84, which was nominally labelled as bottom-limited (see Table 1) and certified by ESTI as such at the beginning of the RR (see CB in Table S2). However, this cell showed CB closest to unity among the three MJ DUTs and even a change in the limiting junction at the end of the RR according to ESTI final verification (not shown here). This might have influenced some of the laboratories' results, especially in those cases where a complete correction for all spectral contributions to the I–V measurement was either not accurately or not at all performed. The EU and ES values in Figure 6 correspond to the ESTI measurements made at the end of the RR PT before and after the pre-conditioning, respectively. The light-blue-shaded area helps in separating them from the results of the RR PT participants, too.

Coming to the results, four participants out of 13 (from #7 to #10) submitted results for P_{max} that agree with the RMPT value because the submitted value itself is within the RMPT value's UC band. Of the other nine laboratories, laboratory #6 submitted a P_{max} value that is beyond the UC band of the RMPT value and whose stated UC intersects that band. However, the overlap of the UCs is not enough to achieve agreement with the RMPT value because the E_n number that can be calculated is −1.1. Moreover, as the disagreement of #6 in I_{SC} is significant (−6.2%) and only partly compensated by the opposite disagreement in *FF*, it is strongly recommended that this laboratory verifies the correctness of the MJ testing procedure as applied here. Laboratory #11 submitted a value for P_{max} that is 0.2% above the UC band of the RMPT value, but it did not submit any UC. However, looking at the agreement (−0.5%) of the submitted I_{SC} with respect to the relevant RMPT value, there seem not to be significant issues with the spectral components at I_{SC} conditions, but rather some cause that influenced the *FF* measurement. For MJ PV devices, though, it has to be noted that the *FF* is also connected to a correct balancing of the spectral components of the solar simulator's light and this is even more relevant if no check is done on the basis of the actual spectrum used for the I–V measurement and of the actual SRs of the DUT and RC. Two other laboratories (#5 and #12) are within the arbitrary threshold of ±5% of the RMPT P_{max} value, but they also show significant deviation in I_{SC}, which may identify the need to check the measurement procedure and/or the calibration value of the RC(s). The remaining five laboratories submitted results that fall outside the ±5% threshold, although for most of them a reasonable UC estimate would make the submitted value of P_{max} cross it, as it happens for #3 and #13. However, for all of them, the strong deviation in P_{max} is either directly connected to a similar significant deviation in I_{SC} or to a combination of the latter with an important deviation in *FF*. This requires a careful analysis of the SR of the actual devices involved in the testing, especially if the DUT shows current limitation of one junction less pronounced than expected, as might have been the case here. Finally, the P_{max} change for this cell during the RR PT was of +0.9% (EU in Figure 6), on the basis of the measurements performed at ESTI when the cells returned there at the end of the RR PT and before further stabilisation. The P_{max} value measured at ESTI after the additional stabilisation was −2.0% of the RMPT value (ES in Figure 6), which can be partly related to the change found in the

limiting-junction for this DUT. This value is indeed at the limit of the agreement with the RMPT value according to the E_n number calculation (E_n = −1.0).

3.1.5 | RR85 (a-Si/µc-Si MJ DUT)

Figure 7 shows the results for RR85, which was nominally a matched cell (see Table 1) and certified by ESTI as top-limited at the beginning of the RR (see CB in Table S2). The EU and ES values correspond to the ESTI measurements made at the end of the RR PT before and after the pre-conditioning, respectively. The light-blue-shaded area helps in separating them from the results of the RR PT participants, too. For this cell, only two laboratories (#5 and #6) out of 13 participants submitted results that agree with the RMPT P_{max} value and its UC band. However, among these two, laboratory #5 shows a significant deviation (−6.0%) in I_{SC} which is just compensated by an opposite deviation in *FF*, thus resulting in the agreement in P_{max}. This laboratory should analyse whether the causes for this deviation can be traced back to an incorrect procedure in the (either *a posteriori* or *a priori*) spectral correction for this DUT. Among the remaining laboratories, six submitted results for P_{max} that are within the arbitrary threshold of ±5% of the RMPT value. If we look at them jointly with the deviation in I_{SC}, laboratories #4, #7 and #8 are outside the UC band of the RMPT P_{max} value (−0.4%, +0.4% and +0.8%), but also have submitted I_{SC} values that are within the UC band of the relevant RMPT value. In addition, the submitted *FF* values do not fall within the UC band of the relevant RMPT value, but it is reasonable to assume that in all cases a sensible UC estimate associated with both P_{max} and *FF* might make these results agree with the RMPT value. A similar reasoning might be partly applicable to laboratory #9 and partly to laboratories #3 and #10; however, for all of them, the deviation in P_{max} is accompanied by a similar deviation in I_{SC}, which might be sign of incorrect or incomplete evaluation of the spectral correction.

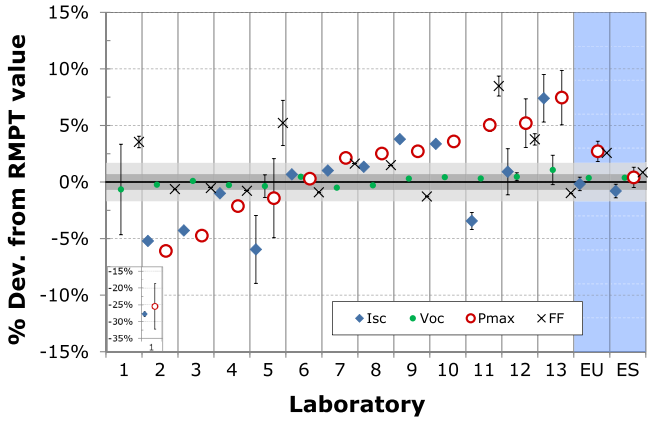


FIGURE 7 Percentage deviations from ESTI RMPT value for I_{SC}, V_{OC}, P_{max} and *FF* of RR85 (a-Si/µc-Si). RMPT value is represented by the *x*-axis and its combined expanded UC (k = 2) is shown for simplicity only for P_{max} (light-grey-shaded area) and *FF* (dark-grey-shaded area). The error bars shown represent the UC of the submitted result as stated by the participant. An inset is shown for the points falling outside the main range of the deviations. The EU and ES values correspond to the ESTI measurements made, respectively, before and after the pre-conditioning at the end of the RR PT. Note that the laboratory identification number may be different for the other DUTs [Colour figure can be viewed at wileyonlinelibrary.com]

The last five laboratories are all outside the arbitrary threshold of ±5% of the RMPT value, although laboratory #11 is just across it (+5.0%). However, this laboratory submitted UC together with the results (UC of P_{max} hidden by the marker's size), and they are not sufficient to cover the deviations from the RMPT values. Therefore, it should analyse in more detail the causes at the origin of the resulting deviations, as they could likely derive from incomplete or incorrect spectral correction (either *a posteriori* or *a priori*), also looking at the deviation in I_{SC} and *FF*. The deviation of laboratory #12 in P_{max}, instead, is not connected to a similar deviation in I_{SC}, which shows good agreement with the RMPT value, but essentially to the one in *FF*, which might indicate issues with the connections together with an incorrect balancing of the two relevant components of the spectral irradiance. For the remaining three laboratories (#1, #2 and #13), the deviation in P_{max} is evidently associated to a similar deviation in I_{SC}, thus suggesting that these laboratories, as others to minor extent, should carefully evaluate their procedures and/or calibration value of the RC(s) for MJ testing.

The change in P_{max} of this DUT during the RR PT was +2.7% (EU in Figure 7), on the basis of the measurements performed at ESTI when the cells returned there at the end of the RR PT and before further stabilisation. The P_{max} value measured at ESTI after the additional stabilisation was +0.4% of the RMPT value (ES in Figure 7), well within the UC of the measurement. Again, no laboratory of those outside the ±5% threshold can sensibly explain the deviation from the RMPT value in relation to its positioning within the temporal sequence of the RR PT.

3.2 | SR measurements

Only a qualitative comparison was made for the SR of the DUTs because of the absence of results for some participants and, more importantly, because most of those available were submitted without UCs. The comparison is shown in the following as normalised EQE plots. The latter do serve to compare the qualitative agreement of the shape of the measured EQE (or SR) to the ESTI SR reference measurement, but they cannot be used to derive quantitative information on the SR of the DUTs in terms of absolute units. The shape of the EQE is enough, though, to evaluate the SMM correction of the I–V curve measurements for SJ PV DUTs; it is only one piece of the necessary information for MJ PV DUTs, for which the limiting junction should be also determined by quantitative assessment. In the same way, they cannot show on their own whether the SR of the DUT was affected in absolute terms by the pre-conditioning or by the long-term degradation of the cells during the entire RR PT. For the MJ PV cells, though,

they can give a visual representation of the relative ratio between the two junctions. Where the laboratory originally measured SR data (as it is the case for ESTI, too) and submitted them as such, the data were converted to EQE values as per:

$$\mathrm{EQE}(\lambda) = \frac{\mathrm{SR}(\lambda)}{\lambda} \times \frac{hc}{q}$$

where λ is the wavelength, h is the Planck's constant, c is the light speed and q is the elementary charge.

In all the graphs, ESTI measured data points are displayed in the same way as in Figure 2 and after conversion to EQE values. The lines between ESTI measured points are just connecting straight lines to help the reader's eye and do not represent any interpolation or any real data. On the contrary, the EQE results from the participant laboratories are shown as lines, because the step in wavelength of the submitted EQE (or SR) results was too short (in some cases even down to 1 nm) to have them represented as discrete points.

The comparison of the normalised EQE data for the SJ PV cells is shown in Figures S3 (RR81, a-Si) and S4 (RR82, μc-Si) in the supporting information. In general, the agreement is good for SJ PV, with only few laboratories that show large deviations from the ESTI measurements in a restricted range of wavelengths. It has to be noted, though, that a quantitative evaluation of these deviations and their effect on the DUT calibration through the SMM correction is not possible here.

In the case of the MJ PV cells, the EQE values of the two junctions have been normalised to the reported maximum value for the bottom junction, so this always reaches 1 while the top junction has a varying intensity, depending on the measured ratio between the values of the two junctions for the three MJ PV DUTs. This choice has been driven by the following considerations:

1. the information on the ratio between the EQE of the two junctions is correctly preserved as submitted by the participants, as opposed to if both individual EQEs were normalised separately;
2. the possible metastability of the μc-Si junction is deemed to be less significant than the one the a-Si junction could have. Therefore, it is used as the relative reference between the two junctions.

Figures 8, 9 and 10 show the comparison for the DUTs RR83, RR84 and RR85, respectively. The graphs also report the results of the measurement performed at ESTI at the beginning of the RR PT before the pre-conditioning of the DUTs (labelled with 2015) in order to give a broader overview of the RR PT results. Indeed, any change in the relative data from ESTI measurements before the start of the RR can highlight possible changes (if any) in the junctions' ratio related only to the pre-conditioning. This information has already been partly discussed in Sections 2.4.2 (DUTs' pre-conditioning at ESTI) and Section 3.1 in terms of the CB values obtained before and after the pre-conditioning; those values are reported in Table S2. Here, the change is shown visual in terms of the EQE shape.

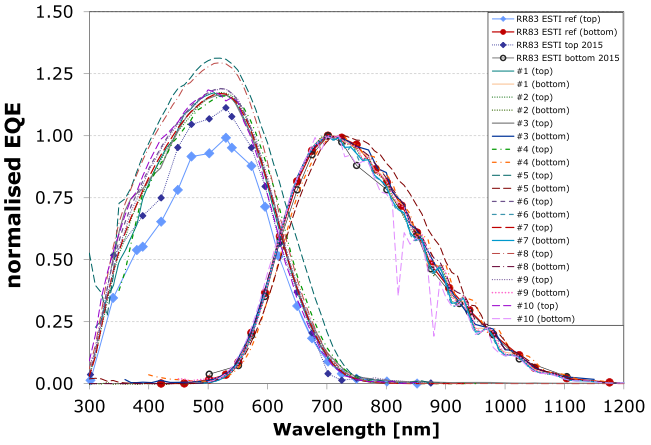


FIGURE 8 Normalised EQE of RR83 (nominally top-limited) for the laboratories that submitted the results. ESTI reference and the data measured before the DUTs pre-conditioning in 2015 are shown, too. The lines connecting ESTI measured points are only shown to help the reader's eye and do not represent any interpolation nor real data [Colour figure can be viewed at wileyonlinelibrary.com]

For all MJ PV DUTs, large deviations from the EQE data calculated from the ESTI reference measurement are visible. As the normalisation of the EQE data is based on the bottom-junction's maximum value, the bottom-junction EQEs show in general a better agreement than the top-junction ones to the ESTI measurement. The agreement in the shape of the bottom-junction EQE is generally observed to be better for RR84 and RR85, while for RR83 the deviation of one laboratory is particularly evident. Another laboratory shows deep holes in the rising slope of the bottom junction, which could be due to enhancement of the interference pattern visible in

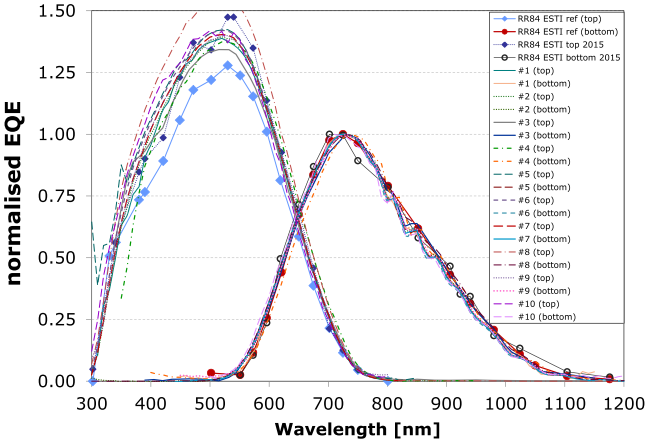


FIGURE 9 Normalised EQE of RR84 (nominally bottom-limited) for the laboratories that submitted the results. ESTI reference and the data measured before the DUTs pre-conditioning in 2015 are shown, too. The lines connecting ESTI measured points are only shown to help the reader's eye and do not represent any interpolation nor real data [Colour figure can be viewed at wileyonlinelibrary.com]

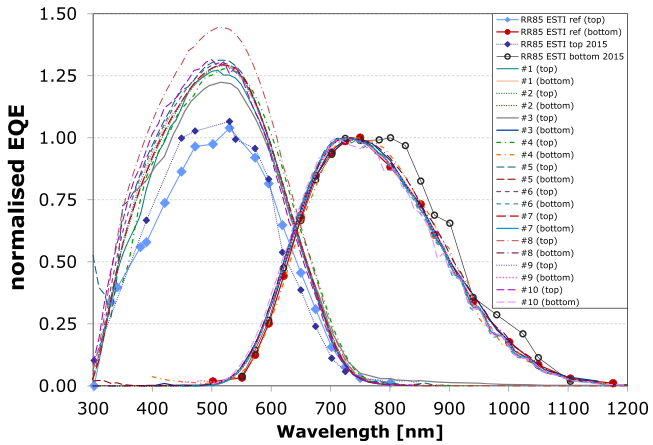


FIGURE 10 Normalised EQE of RR85 (nominally matched) for the laboratories that submitted the results. ESTI reference and the data measured before the DUTs pre-conditioning in 2015 are shown, too. The lines connecting ESTI measured points are only shown to help the reader's eye and do not represent any interpolation nor real data [Colour figure can be viewed at wileyonlinelibrary.com]

the rest of the slope or to contaminations in the optical path. The relative major change in the EQE shape related to the pre-conditioning is visible though for DUT RR85, for which ESTI measurement from 2015 (empty black circles) is significantly away from the reference measurement (red circles), with which the participants mainly agree.

For what concerns the top junction, there is larger variety of results compared to the ESTI reference measurement. In general, all participants submitted relative EQE values with higher ratio to the bottom junction than the ESTI reference measurement has. Without entering a detailed discussion on each participant's measurement, still, it is interesting to note here that the largest deviations are observable for the device RR85 (Figure 10), for which ESTI measured the smallest relative change in the EQE of the top-junction (before and after pre-conditioning measurements) as well as in the ratio between the two junctions of the same device. A larger change in the top-junction EQE, related to the pre-conditioning, is visible for the top-limited device RR83 (Figure 8), as it can be expected. For this device, most of the laboratories have reported EQE values that, when normalised, are slightly above the EQE as calculated from ESTI SR measurements from 2015 (before pre-conditioning). Finally, in the case of the originally bottom-limited DUT (RR84, Figure 9), the observed change in the relative EQE for the top junction calculated from ESTI measurements is sized between the RR83 and the RR85 ones. Also for RR84 and apart from one laboratory, the relative EQE of the top junction reported by the participant laboratories agrees with the data calculated from the initial ESTI measurement, performed before the pre-conditioning, more than with the ESTI reference measurement.

In most of the cases, though, an important cause for the deviations in the SR measurement of the MJ PV cells can be related to the missing or incorrect application of the bias voltage, which is a crucial step in those measurements. This determines not only the correct shape of the SR of the individual junctions but also the correct ratio between them.

3.3 | Key points for good practice in SJ and MJ PV testing

Some important advice and warnings can be derived from the detailed discussion of the results that has been made in the previous sections for both SJ and MJ thin-film PV devices, which were tested during this RR PT. We summarise them here in form of check list:

1. I–V: SMM correction. Good practice for PV testing is to always consider the differences between the measurement conditions and the conditions to which the results have to be reported, for example, STC. A correction either *a priori* or *a posteriori*, if the former is not possible, should be always done, or a component in the UC of the measurement should be included. As a correction has intrinsically always an UC due to the measurements on which it is based, an UC component for the SMM correction should in principle be always included in the overall UC of the PV measurement. This is valid for all PV technologies, regardless of the number of junctions they have.
2. I–V: Actual spectral data. As discussed earlier, the adjustment of the solar simulator is an *a priori* correction for the SMM, to bring the measurement conditions as close as possible to STC. However, as for the analytical *a posteriori* correction of the SMM, it fully works only if the actual spectral data are considered. The latter are in first place the SRs of both the RC and the DUT. This is important even in the case of SJ PV devices, as discussed for RR82 (see Section 3.1.2). The case of a MJ PV device just increases the number of spectral data to be considered, as typically this would imply one RC per junction in the DUT. But actual spectral data include also the actual spectrum under which the I–V measurements are performed, especially if the solar simulator is not adjusted a priori.
3. I–V: Spectral balance. For MJ PV devices, acquires importance the correct balance between the spectral irradiance's components to which the various junctions of the DUT are sensitive. That's why it is essential to use the actual spectral data for both the RCs and each junction of a MJ PV device. For the latter, the correct ratio between the junctions' SRs has to be considered, too. This is necessary to bring the measurement conditions as close as possible to STC, and the verification of the actual spectrum by a measurement should be implemented. Only when this is done, it is possible to correct a posteriori for the residual SMM, in case a fine tuning of the spectrum cannot be performed for any reason. The calculation of the CB value and of the Z factor can help in this.
4. I–V: Reference. It may seem obvious, but a correct calibration and handling of the RC is important, too. For testing laboratories, periodic traceable recalibration of their RCs and intermediate cross-checking of their values are advisable good practices. As well, it is

necessary to evaluate if the selected RC is appropriate for the DUT under measurement or, in case, if an additional SMM correction has to be carried out, either a priori or a posteriori.

5. SR: Bias. The SR measurement of a MJ PV DUT requires the use of an adequate bias light together with an adequate bias voltage. The bias light has to be chosen preferably without emission bands at wavelengths for which the junction under test is responding; it has to be applied to activate the junction(s) not under test much more than the one under test and to make the junction to be tested limiting the current through the device. The bias voltage is needed to bring and keep the junction under test in short-circuit conditions. Depending on the actual device, it is possible that a large range of values for the bias voltage (including zero) produces the correct condition in the DUT; however, as this cannot be known a priori, it is recommended to always verify what value of the bias voltage should be applied.
6. SR: Reference. The RC used for the SR has to respond on a wavelength range at least equal, but preferably larger, than the one on which the DUT responds. For some SJ and MJ PV technologies that are responsive beyond the c-Si limit of 1200 nm (not the case of this RR PT), this could require the use of more than one RC. Extreme care must be used when merging the spectral data from the two sets of measurements acquired with the different RCs.
7. Stabilisation. As partly shown also in this work, a correct stabilisation of unstable or metastable devices, regardless of the number of their junctions, is important for thin-film PV devices. It is recommended to always carry it out according to the relevant international standards and before any testing that has to report the electrical performance of the devices at STC or other agreed testing conditions.

4 | CONCLUSIONS

A RR PT involving 13 participant laboratories, plus the JRC ESTI as the reference laboratory, was run within the European FP7 CHEETAH project. To our knowledge, this is the first completed RR on STC testing of MJ PV devices specifically carried out for non-concentrating terrestrial PV and with such a large number of participating laboratories. The major aim of the RR PT was to evaluate whether the facilities and the procedures for MJ PV testing as applied by the participants were adequate or needed to be revised and improved. A detailed analysis of the submitted results has been reported here, although the deviations from the RMPT values have been mainly presented in terms of percentage difference from the RMPT value due to missing UC information from most participants. A discussion of the STC testing for each DUT has been given, too, highlighting the possible causes at the origin of some poor agreement with the RMPT value as well as areas where each laboratory can improve its measurement procedure and facilities. A summary section (Section 3.3) with good-practice guidelines for SJ and MJ PV testing is included after the results discussion.

The participant laboratories showed various levels of expertise in the measurements to be performed, also with some variation in the facilities and procedures employed. In general, though, there seems to be a significant need to better verify and improve the spectral irradiance measurement and correction (either a priori or a posteriori), in order to achieve P_{max} values that agree with the RMPT value. This is clearly visible from the graphs shown in Section 3.1, where results of all four main electrical parameters as submitted by each laboratory are reported as percentage deviations from the relevant RMPT value. In particular, in the majority of cases, the deviation in P_{max} is connected to a similar deviation in I_{SC}, which in turn is mainly related to spectral issues and much less to other measurement errors. When such a deviation is beyond the stated UC of the RMPT value and when the E_n number is outside [−1; 1] (where its calculation is possible), a careful review of the measurement procedure (including the UCs estimate) and a verification of the calibration value of the RC(s) used for testing should be carried out. This is certainly valid for the three MJ PV devices, but it has also been highlighted in more cases than expected even for the SJ cells and even when excluding the electrical issue occurred to one of them at one laboratory (which affected the successive measurements).

For the SR measurements, only a qualitative comparison was made in terms of normalised EQE data (i.e., of relative shape of the EQE curve) because many laboratories did not submit or even measure it or, when measured, they did not provide the results with any UC. For the SJ PV cells, the agreement of the normalised EQE data seems good in general. For the three MJ PV cells, where the relative ratio between the two junctions inside the same DUT acquires importance, the deviations from the normalised EQE calculated on the basis of the ESTI reference measurements are more pronounced. The size of such deviations is smallest for the bottom-limited device RR84, for which curiously most laboratories agree with the ESTI initial data obtained *before* (and not after) the DUT pre-conditioning, and is largest for the nominally matched device RR85. The latter was identified by ESTI as top-limited and has shown the smallest change in the ratio between the top-junction and the bottom-junction EQE intensities as well as in their relative values; the shape of the EQE, however, has significantly changed especially for the bottom junction, if we compare ESTI 2015 measurement (i.e., before pre-conditioning) and the reference measurement. SR measurements (not shown here) performed at ESTI at the end of the RR PT and after a further light-soaking of the DUTs confirmed the same relative EQE intensities for the two junctions of all MJ PV DUTs but the RR84, for which a further relative reduction was measured in the top-junction intensity compared to the bottom-junction one. The major source for the disagreement in the SR measurement of the MJ PV may be linked to the missing or incorrect application of the bias voltage, which is a crucial step in those measurements.

Some improvements of the interlaboratory comparison itself are suggested and should be applied as much as possible in the next interlaboratory comparisons. In the first place, the light-soaking procedure as required by the IEC 61215-1-3[44] (for a-Si) should be performed at each laboratory before STC measurements. This is an important step

in metastable thin-film PV assessment, as already shown in the past,[21] and it should be implemented whenever possible, although it requires more effort by the participants and can significantly increase the duration of the RR PT. However, while large changes in the SR of the DUTs should not be expected once they are brought to the stable condition, this cannot be completely excluded for the type of DUTs considered here. Therefore, SR or EQE measurements before and after the light-soaking should be performed for MJ PV devices in order to ensure that the ratio between the junctions did not change.

This RR PT has also made a first step in what should become an increasing and broader measurement comparison exercise on testing and calibration of MJ PV devices, because they can play an important role in the future of PV thanks to the large tunability of the spectral properties of their individual junctions. In principle, such properties might also be optimised for the particular climate profile where the PV devices are meant to be installed. Significant improvement of the results' comparison, and therefore of the MJ PV measurements reliability, is expected to be achieved by full and proper implementation of both IEC standards for MJ PV testing[11,12] at all laboratories.

ACKNOWLEDGEMENTS

The CHEETAH project has received funding from the European Union Seventh Framework Programme (FP7/2007-2013) under Grant agreement 609788. Technical help by Tobias Hänel (HZB) is gratefully acknowledged.

REFERENCES

1. IEC. *IEC 61853 Series. Photovoltaic (PV) Module Performance Testing and Energy Rating*. Geneva: International Electrotechnical Commission; 2011.
2. IEC. *IEC 61853-3. Photovoltaic (PV) Module Performance Testing and Energy Rating—Part 3: Energy Rating of PV Modules*. Geneva: International Electrotechnical Commission; 2018.
3. IEC. *IEC 61853-4. Photovoltaic (PV) Module Performance Testing and Energy Rating—Part 4: Standard Reference Climatic Profiles*. Geneva: International Electrotechnical Commission; 2018.
4. IEC. *IEC 60904-1. Photovoltaic Devices—Part 1: Measurement of Photovoltaic Current-Voltage Characteristics*. Geneva: International Electrotechnical Commission; 2006.
5. IEC. *IEC 60891. Photovoltaic Devices—Procedures for Temperature and Irradiance Corrections to Measured I-V Characteristics*. Geneva: International Electrotechnical Commission; 2009.
6. IEC. *IEC 60904-7. Photovoltaic Devices—Part 7: Computation of the Spectral Mismatch Correction for Measurements of Photovoltaic Devices*. Geneva: International Electrotechnical Commission; 2008.
7. IEC. *IEC 60904-8. Photovoltaic Devices—Part 8–1: Measurement of Spectral Responsivity of a Photovoltaic (PV) Device*. Geneva: International Electrotechnical Commission; 2014.
8. IEC. *IEC 60904-10. Photovoltaic Devices—Part 10: Methods of Linearity Measurement*. Geneva: International Electrotechnical Commission; 2009.
9. IEC. *IEC 60904-3. Photovoltaic Devices—Part 3: Measurement Principles for Terrestrial Photovoltaic (PV) Solar Devices with Reference Spectral Irradiance Data*. Geneva: International Electrotechnical Commission; 2019.
10. Friedman DJ. Progress and challenges for next-generation high-efficiency multijunction solar cells. *Curr Opin Solid State Mater Sci*. 2010;14(6):131-138.
11. IEC. *IEC 60904-1-1. Photovoltaic Devices—Part 1–1: Measurement of Current-Voltage Characteristics of Multi-Junction Photovoltaic Devices*. Geneva: International Electrotechnical Commission; 2017.
12. IEC. *IEC 60904-8-1. Photovoltaic Devices—Part 8–1: Measurement of Spectral Responsivity of Multi-Junction Photovoltaic (PV) Devices*. Geneva: International Electrotechnical Commission; 2017.
13. Meusel M, Baur C, Siefer G, Dimroth F, Bett AW, Warta W. Characterization of monolithic III-V multi-junction solar cells-challenges and application. *Sol Energ Mater sol Cells*. 2006;90(18–19):3268-3275.
14. Tsuno Y, Hishikawa Y, Kurokawa K. Separation of the I-V curve of each component cell of multi-junction solar cells. Paper presented at: Photovoltaic Specialists Conference. Conference Record of the Thirty-First IEEE. 2005.
15. Bücher K. Calibration of solar cells for space applications. *Prog Photovoltaics Res Appl*. 1997;5(2):91-107.
16. ISO. *ISO/IEC 17025:2005 General Requirements for the Competence of Testing and Calibration Laboratories*. Geneva: International Organization for Standardization; 2005.
17. Metzdorf J, Wittchen T, Heidler K, et al. Objectives and results of the PEP'87 round-robin calibration of reference solar cells and modules. Paper presented at: IEEE Conference on Photovoltaic Specialists; 21–25 May 1990, 1990.
18. Rummel S, Anderberg A, Emery K, et al. Results from the second international module inter-comparison. Paper presented at: 2006 IEEE 4th World Conference on Photovoltaic Energy Conference; 7–12 May 2006, 2006.
19. Betts TR, Zdanowicz T, Prorok M, et al. Photovoltaic performance measurements in Europe: PV-catapult round robin tests. Paper presented at: 2006 IEEE 4th World Conference on Photovoltaic Energy Conference; 7–12 May 2006, 2006.
20. Hishikawa Y, Liu H, Hsieh H-H, et al. Round-robin measurement intercomparison of c-Si PV modules among Asian testing laboratories. *Prog Photovoltaics Res Appl*. 2013;21(5):1181-1188.
21. Dirnberger D, Kräling U, Müllejans H, et al. Progress in photovoltaic module calibration: results of a worldwide intercomparison between four reference laboratories. *Measurement Science and Technology*. 2014;25(10):105005.
22. Mihaylov B, Bowers JW, Betts TR, et al. *Results of the Sophia Module Intercomparison Part-1: STC, Low Irradiance Conditions and Temperature Coefficients Measurements of C-Si Technologies*. Paper presented at: 29th European Photovoltaic Solar Energy Conference and Exhibition 2014; Amsterdam.
23. Salis E, Pavanello D, Field M, et al. Improvements in world-wide intercomparison of PV module calibration. *Sol Energy*. 2017;155(Supplement C):1451-1461.
24. Kröger I, Friedrich D, Winter S, et al. Results of the round robin calibration of reference solar cells within the PhotoClass project. *Int J Metrol Qual Eng*. 2018;9:1-6. https://doi.org/10.1051/ijmqe/2018006
25. Monokroussos C, Salis E, Etienne D, et al. Electrical characterization intercomparison of high-efficiency c-Si modules within Asian and European laboratories. *Prog Photovoltaics Res Appl*. 2019;27(7):603-622.
26. Osterwald CR, Anevsky S, Bücher K, et al. The world photovoltaic scale: an international reference cell calibration program. *Prog Photovoltaics Res Appl*. 1999;7(4):287-297.
27. Winter S, Metzdorf J, Emery K, et al. The results of the second World Photovoltaic Scale recalibration. Paper presented at: Conference Record of the Thirty-first IEEE Photovoltaic Specialists Conference, 2005.; 3–7 Jan. 2005, 2005.
28. Müllejans H, Zaaiman W, Dunlop ED. *From Sunlight to Power: The History of Achieving a Globally Harmonised Approach to PV Measurement*. Paper presented at: 36th European Photovoltaic Solar Energy Conference and Exhibition 2019; Marseille.778-782.

29. Ishii T, Otani K, Takashima T, Ikeda K. Change in I–V characteristics of thin-film photovoltaic (PV) modules induced by light soaking and thermal annealing effects. *Prog Photovoltaics Res Appl*. 2014;22(9):949-957.
30. Steiner M, Baudrit M, Domínguez C, et al. *SOPHIA CPV Module Round Robin: Power Rating at CSOC*. Paper presented at: 29th European Photovoltaic Solar Energy Conference and Exhibition 2014; Amsterdam.
31. Steiner M, Siefer G, Baudrit M, et al. Rating of CPV modules: results of module round robins. *AIP Conference Proceedings*. 2016;1766(1):1-6, 040005.
32. SOPHIA. SOPHIA project reporting web page. 2011; https://cordis.europa.eu/project/rcn/108132/factsheet/en
33. CHEETAH. CHEETAH project web page. 2014; http://www.cheetah-project.eu/
34. ISO. *ISO/IEC 17043:2010 Conformity Assessment—General Requirements for Proficiency Testing*. Geneva: International Organization for Standardization; 2010.
35. Accredia. ESTI accreditation web page. http://services.accredia.it/ppadt/detail.jsp?PPADT_DETAIL_CODENTE=3203&ID_LINK=1737&area=310&PPADT_SEARCH_SCHEMA=LAT
36. Lauermann I, Salis E, Gerber A, et al. *A European Thin Film Tandem Device Proficiency Test—Practical Outcomes and Preliminary Results*. Paper presented at: 36th European Photovoltaic Solar Energy Conference and Exhibition 2019; Marseille.649–653.
37. Lambertz A, Finger F, Schropp REI, Rau U, Smirnov V. Preparation and measurement of highly efficient a-Si:H single junction solar cells and the advantages of μc-SiOx:H n-layers. *Prog Photovoltaics Res Appl*. 2015;23(8):939-948.
38. Lambertz A, Smirnov V, Merdzhanova T, et al. Microcrystalline silicon–oxygen alloys for application in silicon solar cells and modules. *Sol Energ Mater sol Cells*. 2013;119:134-143.
39. IEC. *IEC 61646. Thin-Film Terrestrial Photovoltaic (PV) Modules—Design Qualification and Type Approval*. Geneva: International Electrotechnical Commission; 2008.
40. IEC. Project: IEC 60904-1-1:2017 ED1. 2017; https://www.iec.ch/dyn/www/f?p=103:38:2857295116853::::FSP_ORG_ID,FSP_APEX_PAGE,FSP_PROJECT_ID:1276,20,21079
41. IEC. Project: IEC 60904-8-1:2017 ED1. 2017; https://www.iec.ch/dyn/www/f?p=103:38:2857295116853::::FSP_ORG_ID,FSP_APEX_PAGE,FSP_PROJECT_ID:1276,20,21075
42. Salis E, Pavanello D, Trentadue G, Müllejans H. Uncertainty budget assessment of temperature coefficient measurements performed via intra-laboratory comparison between various facilities for PV device calibration. *Sol Energy*. 2018;170:293-300.
43. Ebner B, Agostinelli G, Dunlop ED. *Automated Absolute Spectral Response Characterization for Calibration of Secondary Standards*. Paper presented at: 16th European Photovoltaic Solar Energy Conference and Exhibition; May 1-5, 2000; Glasgow, UK.
44. IEC. *IEC 61215-1-3. Terrestrial Photovoltaic (PV) Modules—Design Qualification and Type Approval—Part 1–3: Special Requirements for Testing of Thin-Film Amorphous Silicon Based Photovoltaic (PV) Modules*. Geneva: International Electrotechnical Commission; 2016.
45. IEC. *IEC 61215 Series. Terrestrial Photovoltaic (PV) Modules—Design Qualification and Type Approval*. Geneva: International Electrotechnical Commission.
46. Monokroussos C, Etienne D, Ha J, et al. *Electrical Performance Characterisation Intercomparison of High Efficiency c-Si PV Modules within European and Asian Laboratories*. Paper presented at: 32nd European Photovoltaic Solar Energy Conference and Exhibition 2016; Munich.
47. Balenzategui JL, Cuenca J, Rodríguez-Outón I, Chenlo F. *Intercomparison and Validation of Solar Cell I-V Characteristic Measurement Procedures*. Paper presented at: 27th European Photovoltaic Solar Energy Conference and Exhibition 2012; Frankfurt.
48. Meusel M, Adelhelm R, Dimroth F, Bett AW, Warta W. Spectral mismatch correction and spectrometric characterization of monolithic III-V multi-junction solar cells. *Prog Photovoltaics Res Appl*. 2002;10(4):243-255.

SUPPORTING INFORMATION

Additional supporting information may be found online in the Supporting Information section at the end of this article.

How to cite this article: Salis E, Gerber A, Andreasen JW, et al. A European proficiency test on thin-film tandem photovoltaic devices. *Prog Photovolt Res Appl*. 2020;28:1258–1276. https://doi.org/10.1002/pip.3322

APPENDIX A.

A brief summary of the measurement procedures and facility capabilities at the time of the RR PT is given in the following for the 13 participating laboratories, alphabetically sorted by laboratory's acronym. This sorting has been chosen to preserve as much as possible the anonymity of the reported results, while giving some information on the capabilities of each laboratory. The order of appearance in this list is therefore not connected in any way neither to the actual temporal sequence of the RR PT nor to the actual scoring of the laboratories as reported in this paper.

A.1 | AIT (Austria)

The procedure to attain STC for I–V measurement was done a priori, by adjusting both intensity and spectrum of the solar simulator with a spectrally-matched RC. Therefore, no specific measurement of the EQE was used. In detail, the SMM of solar simulator and DUTs was corrected by an outdoor precision measurement of I_{SC} of the relevant DUT. This was done at a roof top measurement site at AM1.5, stable clear-sky conditions and after the temperature of the devices stabilised. The STC measurement was done with a static solar simulator with shutter (only exposure for measuring I–V) for guaranteeing not to pre-condition the DUTs by parasitic illumination prior to measurement. The I–V characteristics themselves were taken with a delay after shutter opening set to 5 s.

A.2 | CEA-INES (France)

Before acquiring the I–V curves, the total intensity of the solar simulator was adjusted by the reading of a calibrated c-Si RC. No spectral correction was applied. The EQE of the DUTs was measured by a commercial setup and lock-in technique. The ambient light of the room was used as bias light for both SJ DUTs, and no bias voltage was applied. For the tandem cells, bias light (a 630-nm long-pass filter

for the top junction and a 650-nm short-pass filter for the bottom one) as well as bias voltage (0.7 V for the top junction and 0.8 V for the bottom one) were applied.

A.3 | CIEMAT (Spain)

The testing procedure included both I–V curves and EQE measurements. The same c-Si RC traceable via Fraunhofer Institute for Solar Energy Systems ISE (Fraunhofer-ISE) was used for both types of measurement. I–V curves were measured with a Xenon continuous solar simulator operated in pulse mode,[47] whose total irradiance was adjusted to 1000 W/m^2 with the RC. The spectral irradiance was measured by a Licor spectroradiometer between 300 nm and 1180 nm. The submitted values for the electrical parameters were calculated as the average of four I–V curves, every curve measured in a 100-ms pulse. DUT temperature was also controlled and measured.

EQE measurements were done in an in-house designed setup based on a JY TRIAX monochromator and two lamp sources (xenon and tungsten halogen). DUT EQE was measured under over-illumination from 300 nm to 1200 nm. After checking for the DUT operating point under different light sources, it was decided not to apply bias voltage for any of the DUTs. The DUT was kept at short-circuit conditions by connecting it to a trans-impedance amplifier. Two different bias-light sources were used: a blue LED peaked at 450 nm, for which the RC gave an I_{SC} equivalent to 300 W/m^2, and a dichroic lamp with a long-pass filter (cut-off at 760 nm), for which the RC gave an I_{SC} equivalent to 100 W/m^2.

A.4 | CREST (United Kingdom)

The testing procedure included both I–V curve and SR measurements. The latter were performed under over-illumination, without bias voltage even for MJ PV cells and under a bias light of less than 100 W/m^2 in case only narrow-band lights were switched on to bias the junction not under test. The spectral irradiance under which the I–V curves were performed was measured by a spectroradiometer and was used together with the SR data of each DUT to calculate the relevant SMM. The latter was used to correct the I_{SC} of the measured I–V curves as per IEC 60904-7.[6] In the case of the three MJ PV cells, the SMM of the limiting junction was applied.

A.5 | DTU (Denmark)

The testing procedure included both I–V curve and EQE measurements. Before I–V measurements, the total irradiance was adjusted to 1000 W/m^2 by using a c-Si reference device. The measured data were then corrected for the corresponding SMM, which was calculated for each DUT and between 300 nm and 900 nm (due to spectra measurement limitation) on the basis of the EQE measurements. The latter were performed in under-illumination (or spot) mode. For the two SJ cells, white bias light of about 500 W/m^2 produced by halogen lamps and no bias voltage were applied. For the tandem cells, the appropriate bias light was produced by filtering the light from the halogen lamps with bandpass filters around 770 nm to measure the top junction and around 380 nm to measure the bottom one. Bias voltage was applied during the EQE measurement of the tandem cells corresponding to the V_{OC} of the junction chosen as not limiting the cell current.

A.6 | ECN–TNO (The Netherlands)

For all but one DUT, the I–V curves were measured after adjusting the double-lamp solar simulator by use of two RCs, one responsive within [300; 800] nm and the other within [600; 1100] nm. For the μc-Si cell (see Section 2.1), the adjustment was made by using one broadband RC. An average out of three I–V curves was used to calculate the final value of the electrical parameters for each DUT. SR measurements were performed in spot mode against two reference diodes, one used for wavelengths between 300 nm and 1000 nm and the second within (1000; 1100) nm. LEDs were used as bias light for the three tandem DUTs, with wavelength at 735 nm to measure the top junction and at 530 nm to measure the bottom one. Bias voltage was not applied to the tandem cells in the SR measurements.

A.7 | ENEA (Italy)

The I–V curves were measured under a class AAA double-lamp steady-state solar simulator, whose spectral irradiance is periodically monitored. Before the measurements, the total irradiance was adjusted based on a c-Si RC. The average of five consecutive measurements was used as final value for the comparison. The EQE data were measured with lock-in technique in spot mode (spot area of 1.5 × 1.5 mm^2) between 300 nm and 1100 nm against a c-Si RC. Specific bias light condition, obtained by quartz halogen lamps, was applied to each cell type: white bias light for a-Si, no bias light for μc-Si and appropriate filtered light to measure the top (red long-pass filter to bias the bottom junction) and the bottom (blue bandpass filter plus IR-rejecting filter) junctions of the tandem cells.

A.8 | Fraunhofer Institute for Solar Energy Systems ISE (Germany)

The EQE of all cells was measured using a double-grating monochromator with a beam spot smaller than the active cell area. Additional spectrally shaped bias light was used for the tandem devices to measure the EQE of the individual junctions. The I–V curves were measured under a multi-source solar simulator, whose spectral irradiance was adjusted for each junction by adjusting single lamps.[48]

A.9 | HZB (Germany)

The I–V curves were measured under a double-lamp steady-state solar simulator, whose spectral irradiance and spatial non-uniformity is periodically measured. Before the I–V measurements, the total and spectral irradiance of the solar simulator was adjusted by using two c-Si RCs, one provided with a BG40 filter (a-Si like SR) and one unfiltered. To determine the RCs current to be targeted under the solar simulator spectrum, a calculation routine was carried out. The latter was based on a set of two SRs that were considered representative of the a-Si/μc-Si double-junction PV technology and obtained independently from the EQE separately measured in this RR PT. The spectral irradiance was then considered adjusted when the RC matching the DUT delivered the calculated value. The median of 20 measurements was used to submit the final value for each electrical parameter. The EQE measurements were performed with a home-built system in under-illumination mode (spot area of about 2 x 3 mm^2) and with lock-in technique. White bias light from halogen lamps was applied unfiltered for the SJ PV cells and the top junction of the tandem cells; it was filtered with a BG39 filter to measure the bottom junction of the tandem cells. Bias voltage was also applied to measure the top (0.4 V) and the bottom (0.5 V) junctions; no voltage was used in the case of SJ PV DUTs.

A.10 | Jülich Research Centre (Germany)

I–V curves were measured at 25° C using a Wacom steady-state solar simulator equipped with two light sources (Xenon arc lamp and halogen lamp in combination with an AM 1.5 filter). Prior to the measurements, the intensity of the solar simulator was adjusted using a RC traceable via Fraunhofer-ISE Freiburg (with different filters). In addition, the spectrum of the solar simulator was measured using a spectroradiometer (CAS140 from Instrument Systems). The non-uniformity of the test plane (10 × 10 cm^2) was determined with a single Si cell from Hamamatsu (cell area: 5.8 × 5.8 mm^2) by mapping. The I–V curves were swept from I_{SC} to V_{OC} and acquired using a Keithley SMU2420.

The EQE measurements were performed using a home-built system in over-illumination mode (Bentham grid monochromator, HMS lock-in system, Xenon lamp). For measurements with bias light, a Schott KL2500 (Halogen) lamp was used for white light, an RG695 filter for red light and a LED light source (470 nm) for blue light. The system was calibrated using a RC from Gigahertz Optik.

A.11 | TUBITAK (Turkey)

The I–V curves were measured under a single-lamp steady-state solar simulator, whose spectral irradiance and spatial non-uniformity is periodically measured. Before the I–V measurements, the total irradiance of the solar simulator was adjusted to 1000 W/m^2 by using a calibrated unfiltered c-Si RC. Spectral irradiance was not specifically measured, and SMM correction was not applied. An average out of 10 I–V curves was used to calculate the final value of the electrical parameters for each DUT. EQE was not measured.

A.12 | UNIMIB-MIBSOLAR (Italy)

The I–V curves were measured under a steady-state solar simulator (550 W Xenon Arc lamp, 6inch× 6 inch collimated beam, Air Mass 1.5 Global Filter). Before the I–V measurements, the total irradiance of the solar simulator was adjusted to 1000 W/m^2 by using a c-Si RC. The DUT temperature was kept constant at 25° C during the measurements thanks to a temperature-controlled vacuum-chuck. The final electrical results reported are the average values of 10 measurements. The EQE data were measured in spot mode between 300 nm and 1100 nm. A silicon detector (traceable via NIST in the wavelength range (200; 1100) nm) was used as reference device for the EQE measurements. Specific bias light was used only to measure the junctions in the tandem cells: blue LED was switched on for the bottom junction measurement, IR light from a filtered halogen lamp was used to measure the top junction. No bias voltage was applied during EQE measurements.

A.13 | ZSW (Germany)

A single lamp steady-state solar simulator (class AAA) was used to measure I–V curves. Spectral irradiance and spatial uniformity of this solar simulator are controlled regularly. Before the I–V measurements, the total irradiance of the solar simulator was adjusted to 1000 W/m^2 using a calibrated c-Si RC. No numerical spectral corrections were made. EQE measurements were not carried out.